Supplementary Information

Hierarchical Design of Nitrogen-doped Porous Carbon Nanorods for Use in High Efficiency Capacitive Energy Storage

Mei Ni,[a] Zhenghong Huang,[c] Xiaoling Zhang,[a]* Jinping Liu,[a] Liang Qiao[a] and Wen Yang[a,b]*

[a]Key Laboratory of Cluster Science of Ministry of Education, Beijing Key Laboratory of Photoelectronic/Electrophotonic Conversion Materials, School of Chemistry and Chemical Engineering, Beijing Institute of Technology, 5 Zhongguancun Road, Beijing 100081, P. R. China.

[b]State Key Laboratory for Modification of Chemical Fibers and Polymer Materials, School of material science and Engineering, DongHua University, 2999 North Renmin Road, Shanghai 201620, China.

[c]Laboratory of Advanced Materials, Department of Materials Science and Engineering, Tsinghua University, Beijing 100084, China.

E-mail: wenyang@bit.edu.cn; Fax: +86-10-68914780

Supplementary Information

Figure S1. SEM images: (a) CP; (b) MiCP-800; (c) MeMiCP-700.

Figure S2. TEM images: (a) MeCP; (b) MiCP-800; (c) MeMiCP-800. HRTEM images: (d) MeCP; (e) MiCP-800.

Figure S3. (a) Raman spectra and (b) XRD patterns of all samples.

Figure S4. (a) XPS spectrum showing the C1s (284.8 eV), N1s (400.0 eV) and O1s (532.9 eV) peaks of the MeMiCP-800. (b), (c), (d) High resolution spectra of the C1s, N1s and O1s peaks of MeMiCP-800.

Figure S5. Thermogravimetric analysis (TGA) curve of MeMiCP-800 from 30°C to 800°C.

Figure S6. (a) Nitrogen adsorption-desorption isotherms and (b) pore size distributions of BP2000. The specific surface area of BP2000 is 1506 m2 g-1.

Figure S7. Electrochemical capacitive behavior of MeMiCP-800 in two-electrode system in 6 M KOH. (a) CV curves of MeMiCP-800 at different scan rates. (b) and (C) Galvanostatic charge/discharge curves at different current densities of MeMiCP-800.

Table S1. Surface concentration (in at%) of the nitrogen and oxygen species for MeMiCP-800 based on the C1s, N1s and O1s XPS spectra.

Table S2. Performance of various carbon-based ECs in aqueous electrolytes. The specific capacitance values of previous representative porous carbon materials shown in this Table are normalized according to the mass of the active electrode materials only without considering the polymeric or conductive additives.

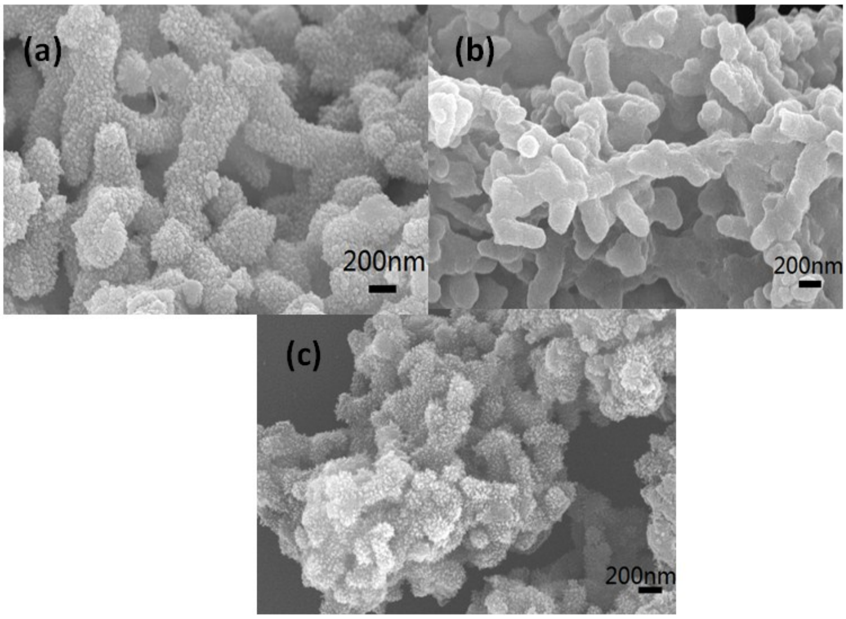

Figure S1. SEM images: (a) CP; (b) MiCP-800; (c) MeMiCP-700.

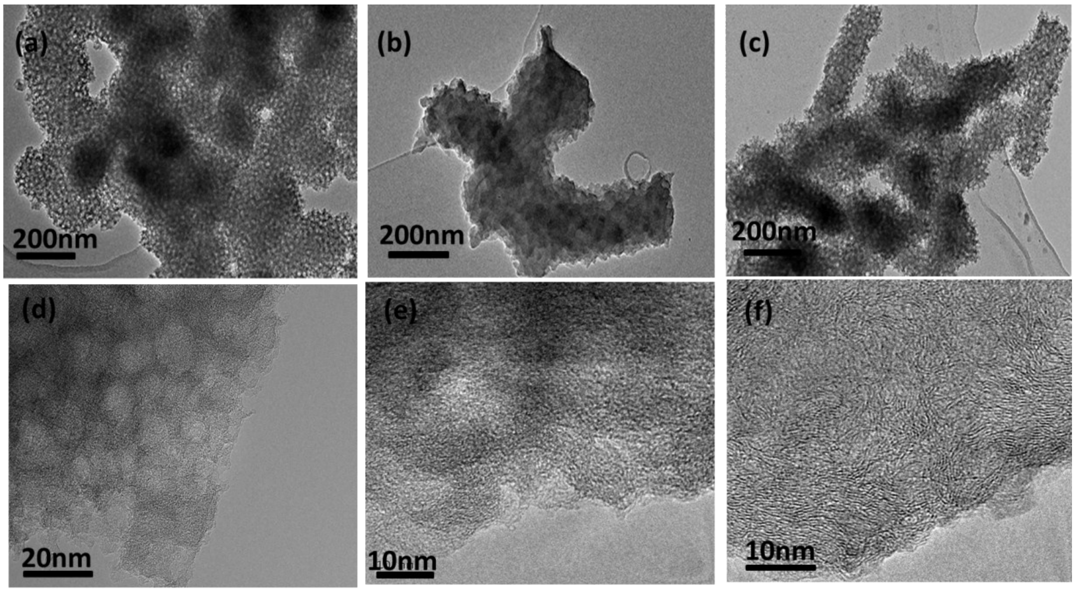

Figure S2. TEM images: (a) MeCP; (b) MiCP-800; (c) MeMiCP-800. HRTEM images: (d) and (e) MeCP; (f) MiCP-800.

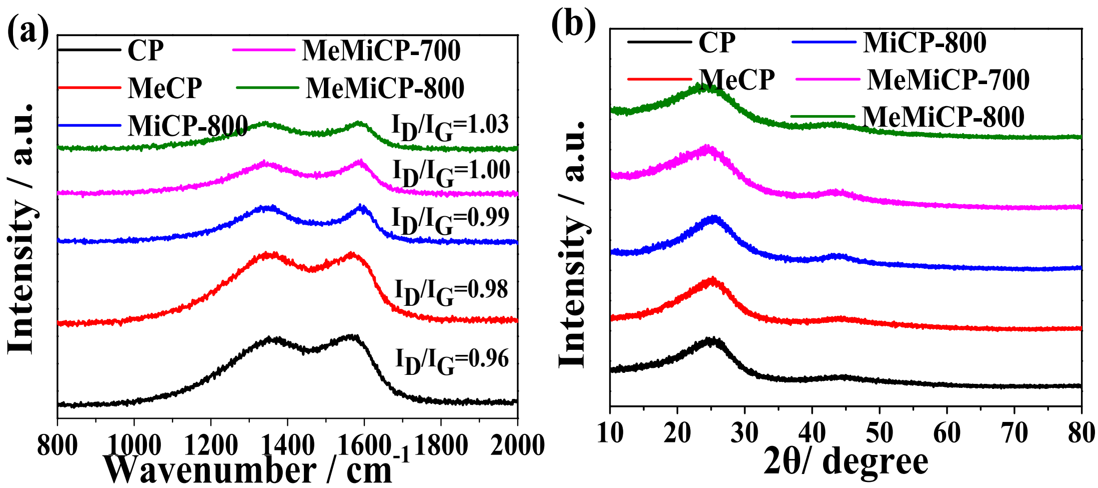

Figure S3. (a) Raman spectra and (b) XRD patterns of all samples.

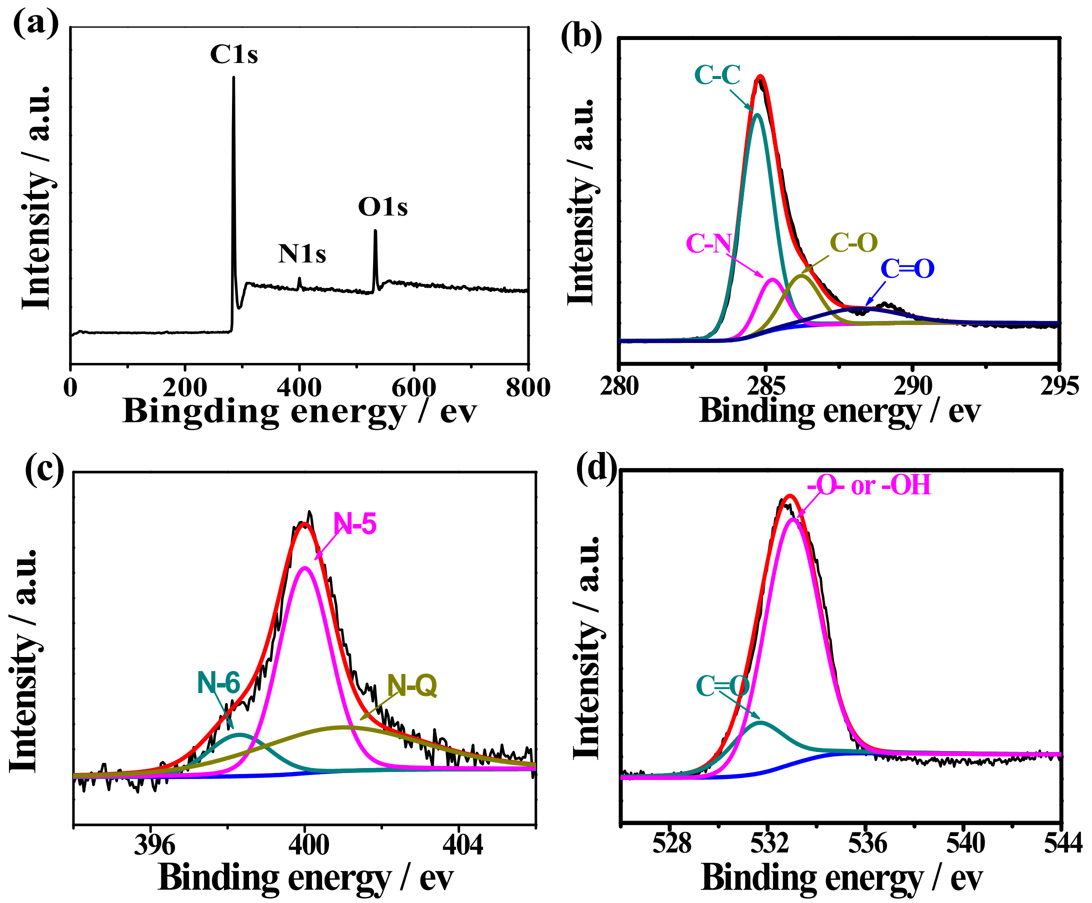

Figure S4. (a) XPS spectrum showing the C1s (284.8 eV), N1s (400.0 eV) and O1s (532.9 eV) peaks of the MeMiCP-800. (b), (c), (d) High resolution spectra of the C1s, N1s and O1s peaks of MeMiCP-800.

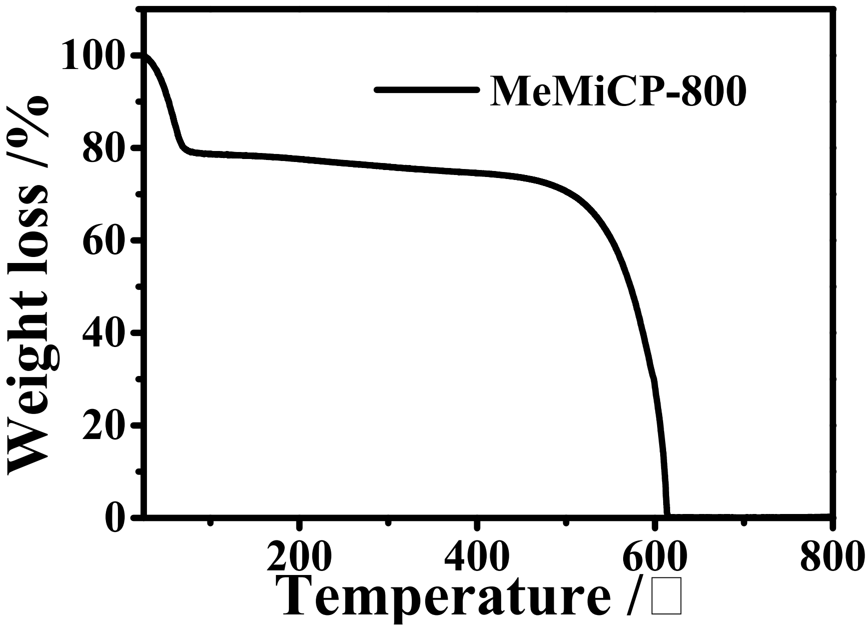

Figure S5. Thermogravimetric analysis (TGA) curve of MeMiCP-800 from 30℃ to 800℃.

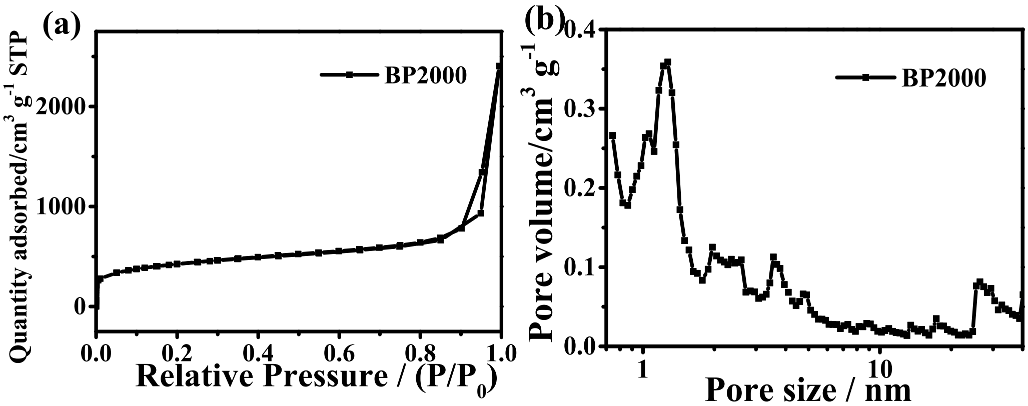

Figure S6. (a) Nitrogen adsorption-desorption isotherms and (b) pore size distributions of BP2000. The specific surface area of BP2000 is 1506 m^2 g^{-1}.

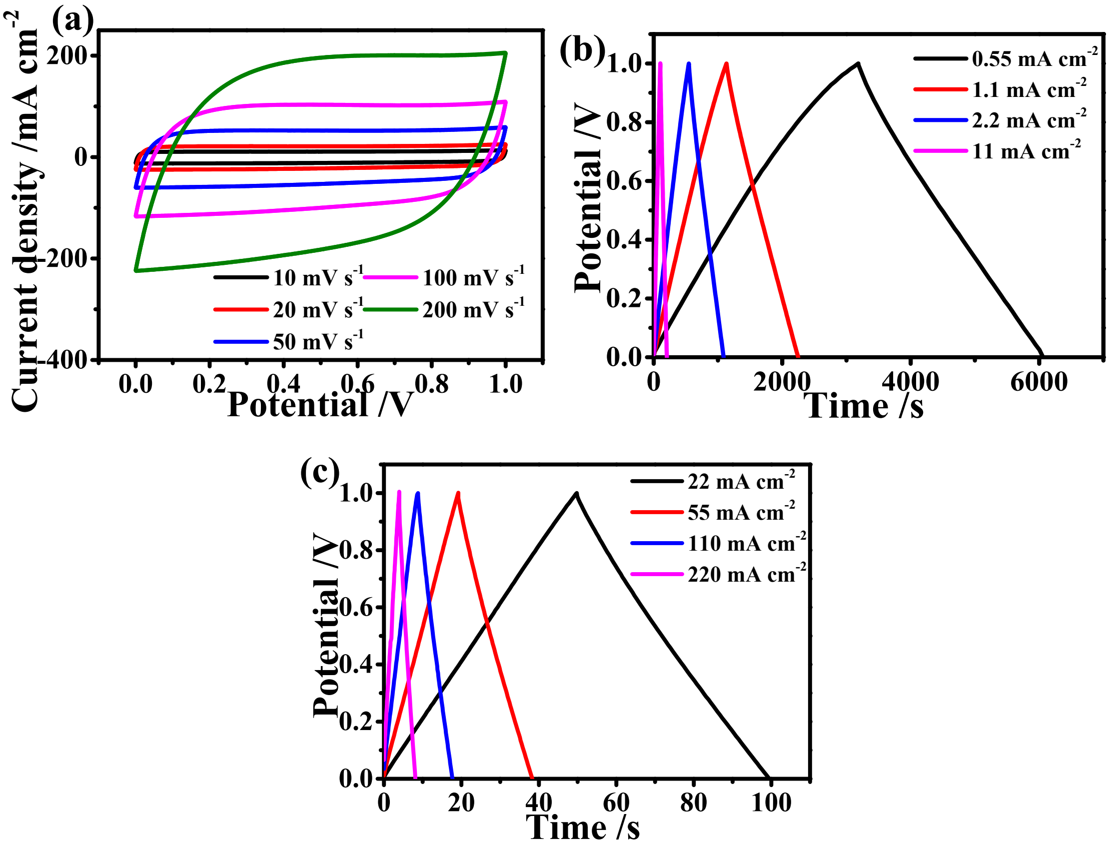

Figure S7. Electrochemical capacitive behavior of MeMiCP-800 in two-electrode system in 6 M KOH. (a) CV curves of MeMiCP-800 at different scan rates. (b) and (C) Galvanostatic charge/discharge curves at different current densities of MeMiCP-800.

Table S1. Surface concentration (in at%) of the nitrogen and oxygen species for MeCP and MeMiCP-800 based on the C1s, N1s and O1s XPS spectra.

Sample	C(%)	N(%)	O(%)	N-6(%)	N-5(%)	N-Q(%)	O-1(%)	O-2(%)
MeCP	82.12	8.95	8.93	30.00	46.20	23.70	30.50	69.50
MeMiCP-800	87.86	2.63	9.51	11.68	51.95	36.37	19.70	80.30

Table S2. Performance of various carbon-based SCs in aqueous electrolytes. The specific capacitance values of previous representative porous carbon materials shown in this Table are normalized according to the mass of the active electrode materials only without considering the polymeric or conductive additives.

Materials reported	Mass loading/mg cm^{-2}	Electrode thickness/μm	Electrolyte (voltage)	C_{wt}/F g^{-1} (current density)	Ref.
Holey graphene	1	14	6 M KOH (1V)	310 (1 A g^{-1})	1
NS-rGO	1.5	—	6 M KOH (1V)	237 (1 A g^{-1})	2
Bio-source-derived carbon sheet	2	—	6 M KOH (1V)	228 (1 A g^{-1})	3
Nitrogen-doped graphitic carbon nanocages	2.2	—	6 M KOH (1V)	248 (1 A g^{-1})	4
Three-dimensional hierarchical porous carbon	3	—	6 M KOH (1V)	236 (2 A g^{-1})	5
Graphene film	4.5	—	6 M KOH (1V)	226 (0.1 A g^{-1})	6
3D hollow porous graphene balls	～5	—	6 M KOH (1V)	321 (0.05 A g^{-1})	7
Highly porous submicron activated carbon fibers	5.66	—	6 M KOH (1V)	196 (50 mv s^{-1})	8
S-porous carbon/graphene	5-7	—	6 M KOH (1.1V)	109 (0.05 A g^{-1})	9
Nitrogen-doped porous carbon	7-9	—	6 M KOH (1V)	281 (0.05 A g^{-1})	10
Porous carbon	—	300	6 M KOH (1V)	262 (0.05 A g^{-1})	11
RGO	～10	—	6 M KOH (1V)	182 (1 A g^{-1})	12
Hierarchical N-doped porous carbon	11	300	6 M KOH (1V)	302(0.05 A g^{-1}) 205(1 A g^{-1})	This work

References

1 Y. X. Xu, Z. Y. Lin, X. Zhong, X .Q. Huang, N. O. Weiss, Y. Huang, et al, N*ature Communications*, 2014, 5, 4554-4562.

2 Y. Yoon, K. Lee, C. Baik, H. Yoo, M. Min, Y. Park, et al, *Adv. Mater.*, 2013, 25, 4437-4444.

3 X. M. Fan, C. Yu, J. Yang, Z. Ling, C. Hu, M. D. Zhang, et al, *Adv. Energy Mater.*, 2014, 1401761-1401767.

4 Y. M. Tan, C. F. Xu, G. X. Chen, Z. H. Liu, M. Ma, Q. J. Xie, et al, *ACS Appl. Mater. Interfaces*, 2013, 5, 2241-2248.

5 L. Qie, W. M. Chen, H. H. Xu, X. Q. Xiong, Y. Jiang, F. Zou, *Energy Environ Sci.*, 2013, 6, 2497-2504.

6 Z. B. Lei, L. Lu, X. S. Zhao, *Energy Environ Sci.*, 2012, 5, 6391-6399.

7 X. J. He, H. B. Zhang, H. Zhang, X. J. Li, N. Xiao, J. S. Qiu, *J. Mater. Chem. A* 2014, 2, 19633-19640.

8 S. X. Hu, S. L. Zhang, N. Pan, Y. L. Hsieh, *J. Power Sources*, 2014, 270, 106-112.

9 M. Seredych, T. J. Bandosz, *J. Mater. Chem. A*, 2013, 1, 11717-11727.

10 B. Xu, H. Duan, M. Chu, G. P. Cao, Y. S. Yang, *J. Mater. Chem. A*, 2013, 1, 4565-4570.

11 B. Xu, F. Wu, S. Chen, Z. M. Zhou, G. P. Cao, Y. S. Yang, *Electrochimica Acta*, 2009, 54, 2185-2189.

12 Y. M. Li, D. Zhao, *Chem. Commun.*, 2015, 51, 5598-5601.

13 L. F. Chen, X. D. Zhang, H. W. Liang, M. G. Kong, Q. F. Guan, P. Chen, Z. Y. Wu, S. H. Yu, *ACS nano*, 2012, 6, 7092-7102.